Received on, 26 March 2025

Accepted on, 10 May 2025

Published on, 15 May 2025

Experimental Investigation on Linear Fresnel Reflector Prototype for Solar Heat Production

Omar Achahour 1*, Badreddine El Ghazzani 2, Rachid Safoui 3, Aicha Eddemani 4, Mohamad Abbassi 5, Abdeslam Elfanaoui 6, and Ahmed Ihlal 7

^{1,2,3,4,6,7} Materials and Renewable Energy Laboratory, Ibn Zohr University, Cité Dakhla, Agadir, Morocco

⁵ Laboratory of Aquatic Systems (AQUAMAR), Faculty of Sciences, Ibn Zohr University, Agadir, Morocco

omar.achahour@edu.uiz.ac.ma, b.elghazzani@yahoo.com, rachid.safoui@edu.uiz.ac.ma, eddemani.aicha@gmail.com, abbassi.mad@gmail.com, a.elfanaoui@uiz.ac.ma, a.ihlal@uiz.ac.ma

ABSTRACT

This paper deals with the conception, design, and construction of a prototype of a Linear Fresnel Reflector (LFR) coupled with a Multi-Effect Distillation system intended for sea-water desalination. Our system consists of 11 flat glass mirrors with a total reflecting surface of 1.5 m² and a tubular receiver-absorber located inside an evacuated glass tube equipped with a secondary reflector. To deal with the discontinuity in heat production, a thermal storage system was built using locally abundant materials such as bedrock. An experimental study of the thermal and optical performances of the system has been assessed to quantify the overall efficiency of our prototype. The salient features of our study include a stagnation temperature as high as 263 °C, the overall heat transfer coefficient reached 22.91 W/m²K, and the estimated collector's efficiency at an operating temperature of 125 °C was 56%. TRNSYS simulation of an LFR system similar to the proposed prototype was conducted. It shows that the system's thermal output is highly influenced by both tank size and flow rate.

Index-words: Linear Fresnel Reflector, Solar Energy, CSP, Thermal storage, optical efficiency.

Nomenclature								
LFR	Linear Fresnel Reflector							
LFC	Linear Fresnel Collector							
CSP	Concentrated Solar Power							
PTC	Parabolic Trough Collector							
TES	Thermal Energy Storage							
MED	Multi-Effect Distillation							
RO	Reverse Osmosis							
DAQ	Data Acquisition System							
HTF	Heat Transfer Fluid							
S	Offset between rows							
d	Distance between adjacent mirror centers							
F	Focal distance							
W _t	Total width of the collector							
W	Width of mirrors							
A_{a}	Collector total area							
A_{r}	Receiver aperture area							
С	Concentration ratio							

Q*	Net solar radiation
q*	Radiation power per unit area
Q_0^*	Radiation incident on the receiver
q_0^*	Incident radiation on the receiver per unit area
Q	Power release to the fluid
α	Absorptivity coefficient
ρ	Reflectivity coefficient
τ	Transmissivity coefficient
IC	Interception factor
η_{opt}	Optical efficiency
η_{th}	Thermal efficiency
$\eta_{\rm c}$	Collector's efficiency
T _r	Receiver temperature
T_0	Ambient temperature
T _{rmax}	Maximum receiver temperature
$T_{\rm stag}$	Stagnation temperature
U _r	Overall heat transfer coefficient
Y	Stagnation parameter

I. INTRODUCTION

Water scarcity has emerged as a serious global challenge, threatening sustainable development and human survival and demanding urgent solutions. Nowadays, two-thirds of the worldwide population suffers from water shortage due to population growth, climate change, industrialization, and water-quality deterioration [1]. It is estimated that more than half of the worldwide population will face clean water scarcity by the 2050s with the growth of the population and the worsening of pollution [2]. MENA region, with more than half of the population having very limited access to drinkable water, is one of the most affected [3][4]. Affording drinking water is then the major challenge for decision-makers. Morocco, particularly the southern part of the country, has shown a scaring water shortage. Even though water management in Morocco is recognized worldwide, the country is facing continuous and growing issues in potable water supply. To alleviate this critical issue, various effective strategies have been implemented to expand freshwater resources in the kingdom, including water transportation from water-abundant regions to deficit ones (North to South), seawater desalination, and water purification technologies. The first method requires heavy investments and presents several risks associated with the continuous drop in water surplus over all regions of the country. Additionally, extending pipelines to transport and deliver clean water over long distances is logistically complex, expensive, and environmentally unsustainable. On the other hand, desalination of salt water is widely employed to meet the demand for freshwater in numerous regions worldwide, particularly in MENA regions. The process of desalination involves extracting dissolved salts from saline water, thereby producing freshwater that is suitable for drinking or other potable uses. The most widely used commercial desalination techniques globally have identified as reverse osmosis (RO), multistage flash (MSF), multi-effect distillation (MED), nanofiltration (NF), and Electrodialysis (ED) [5]. In 2021, the total global desalination capacity was approximately 115 million cubic meters per day, with reverse osmosis technology accounting for around 88 million cubic meters per day, constituting roughly 77% of the total installed capacity [5]. However, the considerable energy demands needed to power desalination systems contribute to elevated costs of desalinated water, potentially compromising the economic feasibility of desalination projects. The energy demands for reverse osmosis desalination processes range from approximately 2 to 5.5 kWh per cubic meter, and electricity expenses constitute nearly 44% of the total costs involved in water production [5],[6],[7],[8]. Using renewable energy to operate desalination systems represents a sustainable approach to supplying potable water in water-stressed regions [9]. Solar energy is the most abundant renewable energy source and is highly suitable for driving both thermal and membranebased desalination processes. Numerous studies have highlighted the significance and appropriateness of solar-powered desalination techniques for the water-scarce Middle East and North Africa region [10]. The coupling of solar energy technologies, such as concentrated solar power and water desalination techniques, is a suitable solution to address the global demand for freshwater [10]. The multi-effect distillation technique exhibits favorable characteristics, such as low energy consumption, extended operational lifespan, and lower capital expenditures, rendering it a competitive option compared to reverse osmosis and multistage flash desalination methods [11]. MED and RO are the most promising desalination technologies for coupling with solar power plants to produce fresh water.

For small to medium-sized applications, Linear Fresnel Collectors (LFCs) have gained significant attention due to their simplicity, cost-effectiveness, and ability to produce suitable heat for MED [12]. Linear Fresnel Reflector systems are characterized by the linear arrangement of mirrors that focus sun rays onto a fixed receiver. These systems offer a promising balance between economic feasibility and efficiency [13][14]. The optical efficiency is higher in parabolic trough collectors compared to linear Fresnel collectors. However, Parabolic Trough Collectors (PTC) plants are significantly more expensive, and their manufacturing process is highly complex [15][16].

Linear Fresnel collector plants are a promising line-focusing concentrating solar thermal method. This technology has been the subject of several scientific studies. Rungsamy et al. [12] conducted a review study on linear Fresnel primary optical design methodologies where they detail the optical loss mechanisms and their relative importance to the performance of the LFR. Ahmadpour et al. [17] have used various methods based on Monte Carlo Ray-Trace to conduct a study on the optimization and the modeling of linear Fresnel reflector solar concentrators. Sun et al. [16] have carried out a comprehensive review of Line-Focus Concentrating

Solar Thermal Technologies in which they have compared PTC and LFR. Alhaj et al. [18] have led an investigation on the Life-Cycle Environmental Assessment (LCA) of an optimized solar-driven Multi-Effect Desalination plant. They realized that the linear Fresnel collector has a better LCA rating than the PTC.

This work demonstrates a comprehensive study on the development and design of a prototype of a small-scale solar power plant based on Linear Fresnel Collectors, developed to be coupled with a Multi-Effect Desalination system [19]. The focus is exclusively on the design of the plant components and their optical optimization, with the aim of achieving a system configuration that maximizes operational efficiency and thermal performance. Some Key design considerations, including solar field sizing, receiver type, the integration of thermal energy storage (TES), and the optimization of operational parameters, are analyzed to achieve a reliable and efficient solar-driven desalination system. The LFR system was designed to feed a MED desalination system. It is worth noting that MED desalination plants are typically sized to treat between 2,000 and 20,000 m³ of seawater per day. These systems significantly reduce scaling and optimize plant operation [20]. The most recent models are designed to operate at first-stage temperatures of around 70°C. Thus, the main goal of our prototype is to produce heat at this range of temperature and above to meet the load demand of MED systems.

The content of our paper is presented as follow; in the first section the prototype is described, and its main components are detailed, the use of a new designed absorber is highlighted, after that the theoretical modeling is depicted. The third section describes the experimental setup and the methodology adopted. Finally, the results are exposed and discussed.

This study aims to contribute to the growing body of research on solar desalination by providing important insights into the practical implementation of LFRs for MED applications.

II. MATERIALS AND METHODS

A. Experimental Setup

Despite the growing interest in Linear Fresnel Reflector (LFR) as a reliable technology for solar thermal applications, most of the existing studies focus on large-scale systems, which generally involve complex infrastructure requirements and relatively significant investment. Otherwise, there is a remarkable gap in the literature concerning the development of economically viable, small-scale LFR systems that can be tailored for decentralized applications, such as coupling with medium-sized Multi-Effect Desalination (MED) units in resourceconstrained or remote regions. This paper addresses this gap by focusing on the design and optimization of a compact and cost-effective LFR prototype, aiming to achieve both high thermal efficiency and economic feasibility. Furthermore, the present work contributes to expanding the applicability of LFR systems beyond large-scale installations, especially for sustainable desalination.

Our experimental study is intended to explore the energy potential of the Fresnel linear reflector system. A designed MED (under construction) was adopted as the most suitable distillation process to be coupled to the LFR system. The prototype was designed, built, and installed at the Materials and Renewable Energy Laboratory (LMER) at the Faculty of Science in Agadir, Ibn Zohr University in Morocco (Latitude: 30°24'22" N, Longitude: 9°32'38" W, Altitude: 73 m). Fig. 1 shows a photograph of the system with all its components. During the realization, we opted for low-cost technological solutions by choosing locally available materials, which will make this system accessible to the general public.



Fig. 1. Picture of the global view of the LFR prototype

Fig.2 shows a schematic diagram of the prototype, including three main components:

- The LFR concentrator with the absorber.
- The storage tank.

 Heat consumption process ("MED distiller," under construction).

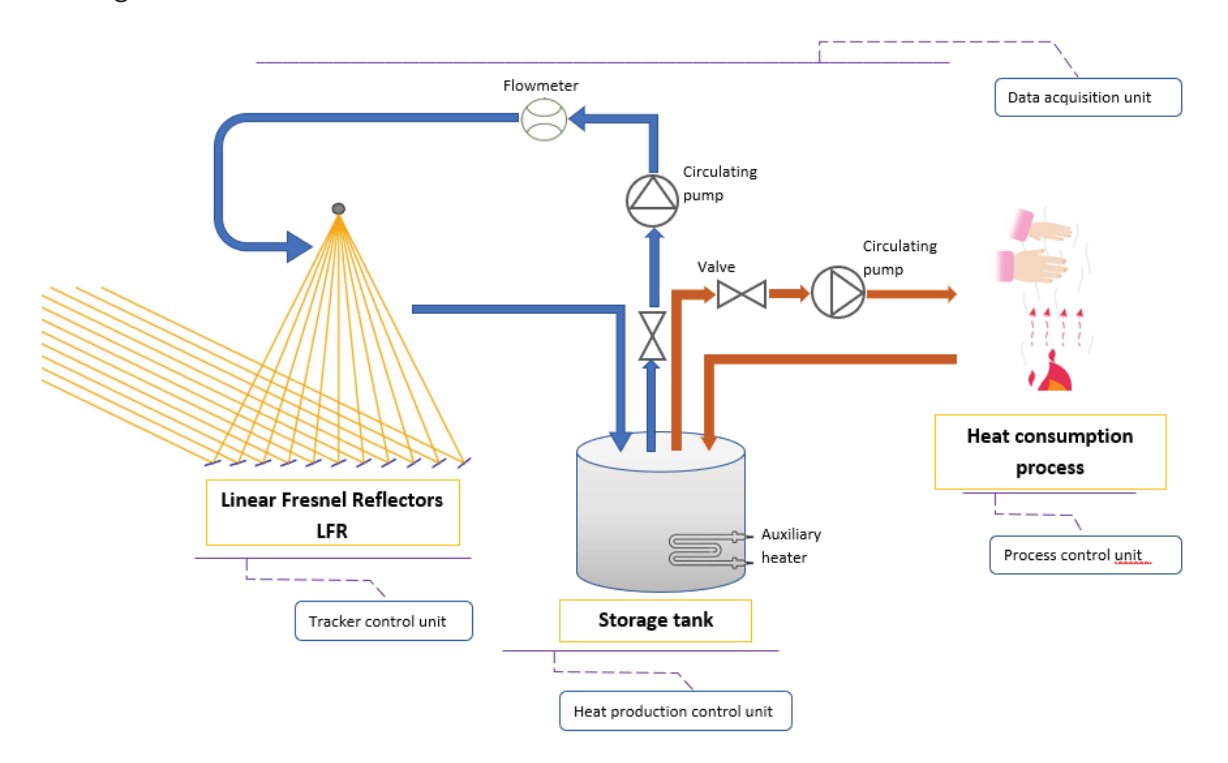


Fig. 2. Diagram of the main components in the prototype

1. LFR system

The LFR structure illustrated in Fig. 3 is made from galvanized iron and carries the primary reflector's mirrors, the receiver, the secondary reflector, and the rotation mechanism that allows the mirrors to concentrate direct solar radiation towards the receiver.

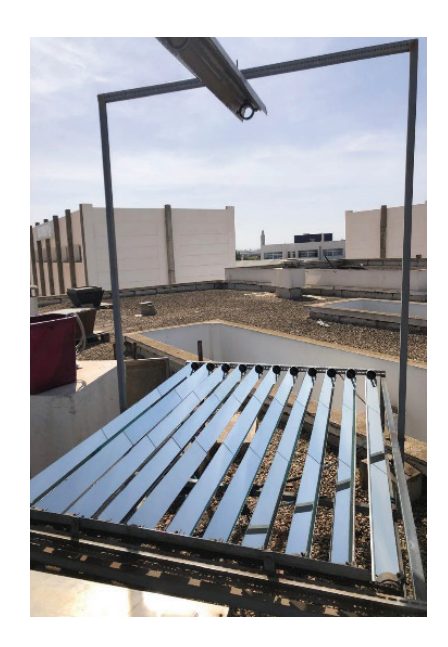


Fig. 3. structure and primary reflector's mirrors

This LFR system features 11 rows of rectangular flat glass mirrors measuring 1800 mm in length, 80 mm in width, and 4mm in thickness. The resulting total reflective surface is 1.58 m². The reflectivity of the flat mirrors is expected to reach 94% [21]. Fig. 4 shows a model of an LFR with 11 flat primary reflectors:

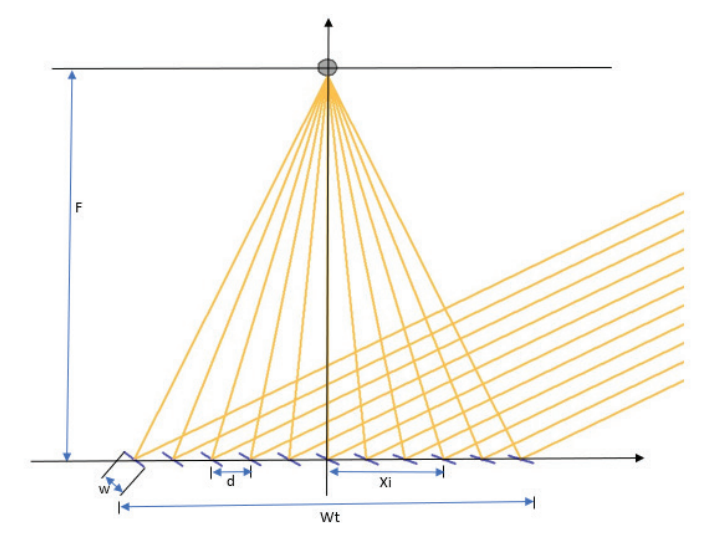


Fig. 4. A model form of an LFR with a flat primary reflector

Based on the equations reported by Mathur [22], to avoid blocking and shading of incident solar radiation between adjacent mirrors, the offset

between rows was set at:

S = d - w = 4 cm. The other dimensions are provided in Table I below:

TABLE I. GEOMETRIC DIMENSIONS OF THE SOLAR COLLECTOR

Dimension	symbol	value
Focal distance	F	145 cm
Total width	Wt	128 cm
Mirror width	w	8 cm
Distance between the middle of adjacent mirrors	d	12 cm

2. The receiver features

The designed tubular absorber is similar to a heat exchanger (Fig.5). It consists of three copper comprise tubes: a main tube with an internal diameter of 1 inch and two thinner tubes with an internal diameter of 1/4 inch, welded back and forth along its outer surface. The heat transfer fluid circulates through the thin tubes, absorbing the heat concentrated by the mirrors. The whole unit is enclosed in a vacuum glass tube. This configuration is expected to minimize heat loss and then improve the efficiency of the system.

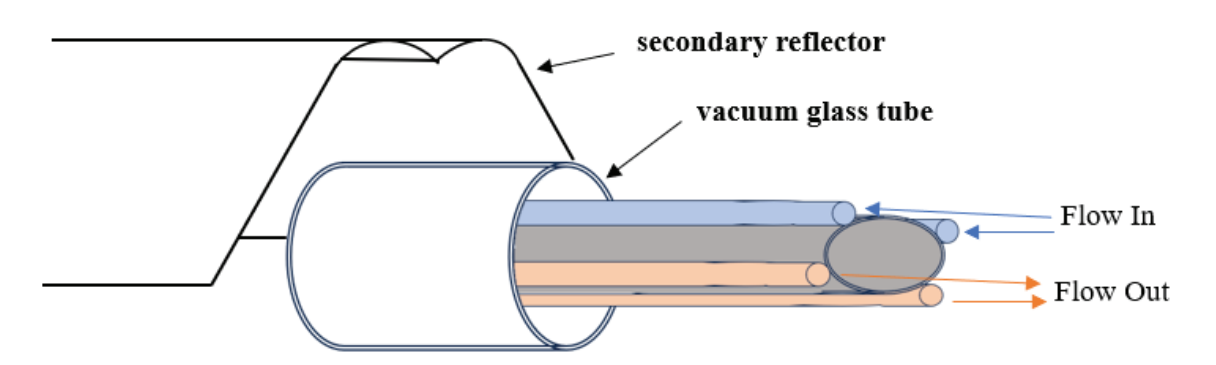


Fig. 5. Schematic of the tubular receiver with the second reflector







Fig. 6. Overview of the receiver components

The HTF selected for this prototype is the synthetic oil called Therminol 62 [25] (temperature range: -23°C to 325°C) to ensure that the system pressure remains low when the operating temperature exceeds 100 °C. The main properties of this oil are thermal conductivity and heat capacity, which are respectively 0.11 W/m·K and 2.2 kJ/kg·K.

3. Heat storage tank

A thermal storage system has been built to mitigate fluctuations in solar energy production and enhance the flexibility of the prototype [24]. Our stainless-steel cylindrical tank has a volume of 37 Liters. To minimize heat loss and maintain a high temperature inside the tank, 3 cm thick fiberglass insulation has been installed (Fig. 7 and Fig. 8).

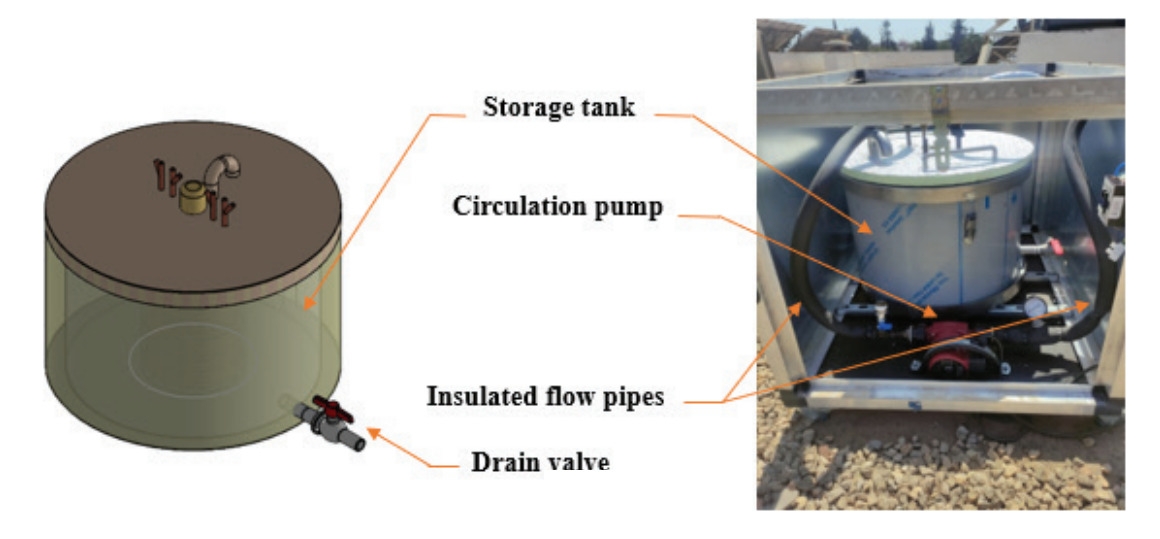


Fig. 7. Overview of the thermal storage tank and circulation circuit components

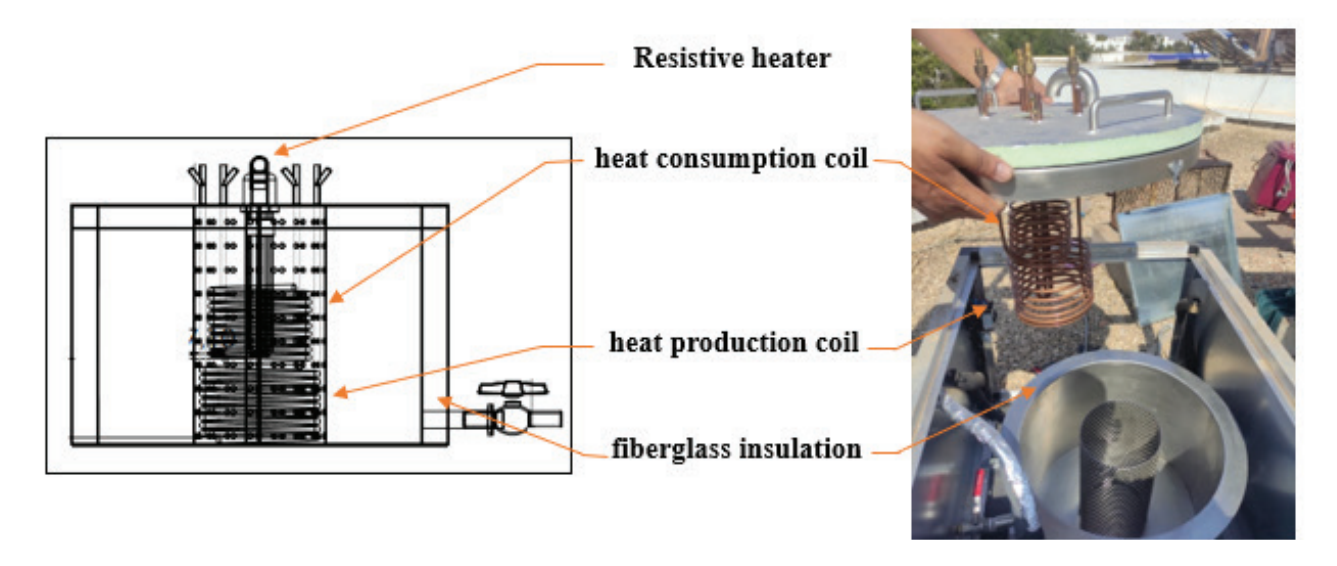


Fig. 8. Internal components of the thermal storage tank

Two helical coils, as a heat exchanger, are equipped in the tank: one dedicated to the heat production circuit (absorber) and the other to the heat consumption circuit. The circulation of heat transfer fluids (HTF) is ensured by a circulation pump.

B. Experimental Method and System Operation

To thoroughly evaluate the performance of the developed Linear Fresnel Reflector prototype, practical experiments were conducted on January 6, 2023. The solar illumination was sufficient to obtain reliable experimental results. The tests were performed from 11:00 AM to 2:00 PM. A comprehensive experimental setup was established, encompassing two distinct experiments:

1. Stagnation temperature determination

The primary objective of this experiment was to determine the stagnation temperature of the LFR prototype. This crucial parameter reflects the system's maximum achievable temperature under no-load conditions and aids in calculating other characteristic parameters of the collector. The experimental setup involved:

- The complete LFR prototype, including the collectors and absorber.
 - Data Acquisition System (Datalogger « OM-DAQPRO-5300 », Fig. 9 was employed to continuously record temperature data from the sensors throughout the experiment. The temperature sensors were strategically placed on the absorber tube surface and in the ambient environment to monitor temperature variations.



Fig. 9. Picture of the Datalogger « OM-DAQPRO-5300 » used for temperature measurement

This device offers a wide measurement range from $-200\,^{\circ}\text{C}$ to $400\,^{\circ}\text{C}$, a resolution of $0.1\,^{\circ}\text{C}$, and a precision of $\pm 0.5\%$ of the reading [26]. These specifications ensure sufficient accuracy for evaluating the thermal performance of the prototype.

The experiments commenced with starting the single axis (North-South) tracking unit of the LFR prototype to maximize direct sunlight interception. The system was allowed to operate for an extended period until a steady-state condition was reached. During this period, the DAQ meticulously recorded the receiver and ambient temperature data every minute. The stagnation temperature was identified as the point where the absorber tube temperature stabilized and exhibited minimal further increase.

2. Optical efficiency measurement

To assess the optical efficiency (η_{opt}) of the LFR prototype, a solarimeter was used to evaluate the direct part of the incident solar radiation. This experiment aimed to quantify the proportion of incident solar radiation effectively captured and redirected by the collector panels. The setup included:

- The LFR prototype is positioned under direct sunlight.
- Data Acquisition System: Solarimeter « TES 132 Datalogging Solar Power Meter » (Fig. 10) was employed to continuously record solar radiation data from the solarimeter.



Fig. 10. Solarimeter « TES 132 Solar Power Meter »

This instrument operates over a range of 200 W/m² to 2000 W/m², with a resolution of 0.1 W/m². Its accuracy is ± 10 W/m², with an additional temperature-induced error of ± 0.38 W/m²/°C [27].

experiment involved the simultaneous measurement of incident solar radiation using a solarimeter. The solarimeter's measurement limit of 2000 W/m² imposed certain experimental constraints, particularly in conditions of strong sunlight. A methodology based on the measurement of incident and reflected solar power on each mirror line was then adopted. This approach takes into account the heterogeneities specific to each mirror and enables the local optical efficiency to be determined. The overall optical efficiency of the reflector is then calculated by averaging the individual efficiencies. This method provides a representative estimation of the system's optical efficiency while also enabling any areas of poor performance to be identified.

C. Theoretical Modeling and Simulation

1. Mathematical modeling

Fresnel linear concentrators use segmental mirror fields with a solar tracking system to focus direct radiation on a tubular receiver. The precision of the angular tracking is a decisive parameter to minimize losses by diffuse reflection and optimize energy concentration. Based on the analysis reported by S. Kalogirou [28], assuming a collector with a total heliostat area (Aa). This collector intercepts solar radiation at a rate of Q^* from the sun, as illustrated in the diagram Fig.11:

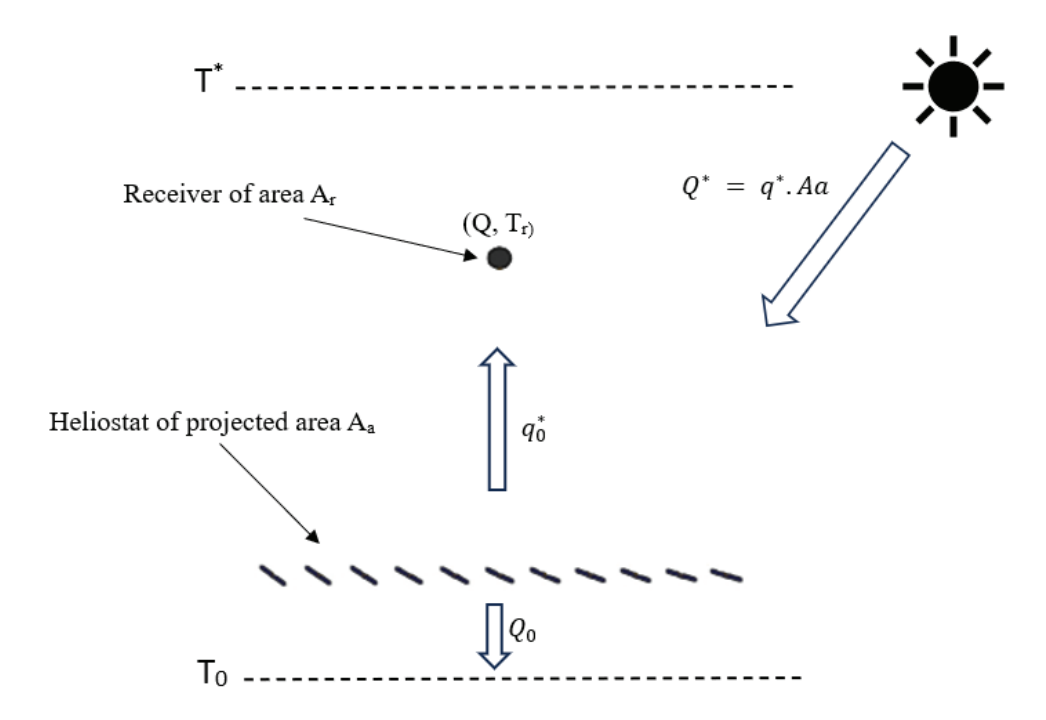


Fig. 11. Modeling of the path of solar energy collected by a linear Fresnel concentrator

Diverse factors such as geographical location, collector orientation, weather conditions, and time of day influence the radiation power per unit area, $q^*(W/m^2)$. Thus, the net solar heat transfer, Q^* , is proportional to q^* and the collector area, Aa. For simplicity, q^* is assumed to be constant, and the system is considered to be in equilibrium.

$$Q^* = q^*.Aa \tag{1}$$

 q_0^* means that the incident radiation on the receiver depends on the optical efficiency. This efficiency accounts for various factors, including the tracking system precision, the optical errors of the mirror (such as its reflectance), and the optical properties of the receiver.

$$\eta_{opt} = \alpha . \rho. t. IC \tag{2}$$

Where:

- η_{opt}: optical efficiency
- α: absorptive coefficient
- ρ: reflectivity coefficient
- τ: transitivity coefficient
- IC: interception factor.

It should be noted that Eq. (2) highlights the theoretical complexity involved in explicitly

determining the optical efficiency η_{opt} from the individual parameters (absorptivity, reflectivity, transmissivity, and interception factor). Given the practical challenges in accurately measuring each of these coefficients experimentally, we opted instead to use Eq. (3). This latter approach allows us to directly quantify optical efficiency by experimentally determining the ratio between the useful radiation transferred to the receiver and the total incident radiation, thus ensuring reliable and reproducible results.

The radiation incident on the receiver is:

$$Q_0^* = \eta_{opt} \cdot Q^* \tag{3}$$

The thermal efficiency of the receiver, $\eta_{\rm th}$, reflects how effectively the incident solar energy is converted into thermal energy at the receiver and transferred to the heat transfer fluid. It quantifies the receiver's ability to absorb heat and deliver it to the fluid. Thermal efficiency is influenced by various factors, including the receiver's temperature, the properties of the heat transfer fluid, the quality of the absorbing surface, and unavoidable thermal losses through convection, radiation, or conduction.

The power release to the fluid is given by:

$$Q = \eta_{th} \cdot Q_0^* \tag{4}$$

The power flow balance shown in the diagram of Fig. 12 points out that a portion of the incident

solar radiation is transferred as heat, Q, to a power cycle (or user) at the receiver temperature, T_r . The remaining fraction, Q_0 , accounts for the heat lost to the ambient environment by the collector. Then, we deduce the following equation:

$$Q_0 = Q^* - Q \tag{5}$$

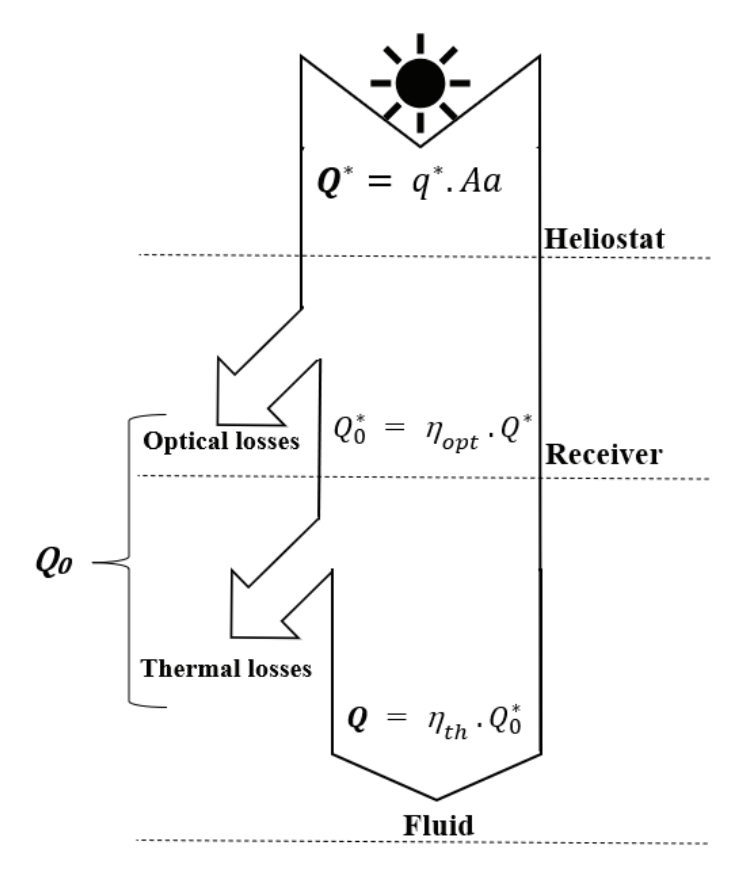


Fig. 12. Power flow diagram

 Q_0 (Englobing the optical and thermal losses) is proportional to the temperature difference between the receiver and the ambient environment and to the receiver aperture area A_r as:

$$Q_0 = Ur.Ar(Tr - T0)$$
 (6)

We have to bear in mind that Ur (characteristic constant of the collector) is the overall heat transfer coefficient based on the receiver aperture area.

The maximum receiver temperature (stagnation temperature), obtained at a no-flow condition, is reached when Q=0. This means that all of the solar heat transfer, Q^* , is lost to the ambient environment.

The Eq. (5) becomes: $Q_0 = Q^*$

Thus, at $T_r = T_{stag} = T_{rmax}$:

By combining Eq. (1) and Eq. (6) with $C = \frac{Aa}{Ar}$:

$$Ur = \frac{q^*.C}{(T_{rmax} - T_0)} \tag{7}$$

The Eq. (7) gives the maximum collector temperature as follows:

$$T_{r\,max} = \frac{q^*.C}{Ur} + T_0 \tag{8}$$

As shown in Eq. (8), T_{rmax} is directly related to C, meaning that a higher collector concentration ratio results in a higher T_{rmax} value. The stagnation temperature serves as a key parameter for evaluating the collector's performance in relation to ambient heat loss. In stagnation conditions, the energy collected balances the energy lost.

The collector's efficiency is given by:

$$\eta_c = \frac{Q}{Q^*} = 1 - \frac{Q_0}{Q^*} \tag{9}$$

Combining Eq. (1) and Eq. (6), we find:

$$\eta_{Hc} = 1 - \frac{U_r A_r (T_r - T_0)}{q^* Aa} = 1 - \frac{U_r (T_r - T_0)}{q^* C}$$
 (10)

Using Eq. (7), the collector's efficiency can be cut down to:

$$\eta_c = 1 - \frac{(T_r - T_0)}{(T_{r max} - T_0)} \tag{11}$$

Therefore, η_c varies linearly with the collector temperature. The concentrator efficiency vanishes at the stagnation point, where heat transfer Q exerts no potential to produce work.

2. Simulation test on TRNSYS

TRNSYS is a dynamic simulation tool for evaluating the performances of energy systems. A simulation using TRNSYS software was conducted to investigate the performance of the LFR prototype under varying conditions. The simulation involved:

- LFR Prototype Model: "Type 1288; Concentrating Collector, EN12975 Dynamic Efficiency Approach". A detailed model of the LFR prototype developed within TRNSYS, incorporating its geometrical characteristics, material properties, and operational parameters.
- Weather Data: "Meteonorm TMY2" Historical weather data for Agadir city in Morocco was obtained and incorporated into the simulation.

 Simulation Scenario: Various simulation scenarios were defined, encompassing different seasons, weather conditions, and solar radiation patterns. The layout of the TRNSYS simulation conducted is illustrated in Fig. 13. The aim is to predict the performances of the LFR prototype under various scenarios, providing insights into its long-term behavior and energy yield potential.

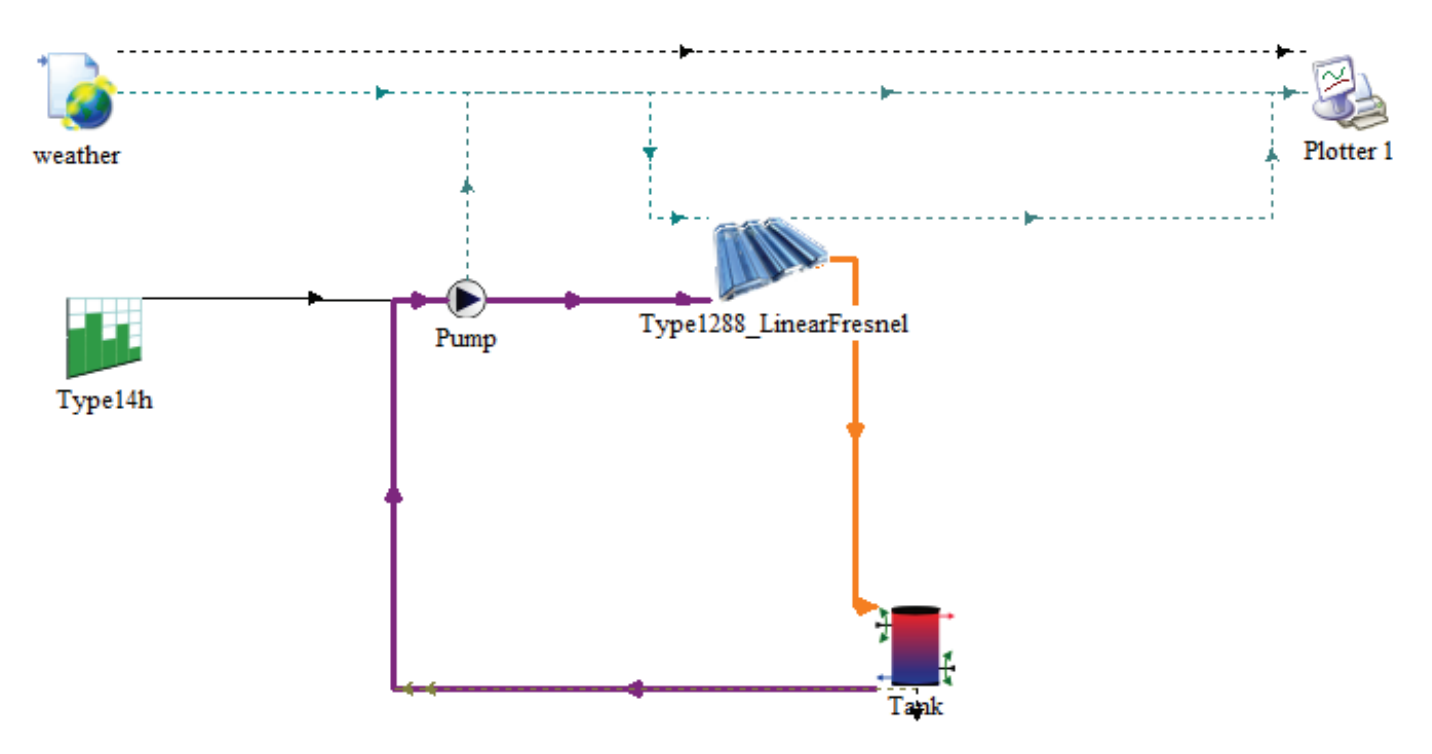


Fig. 13. Diagram of the LFR system simulated in TRNSYS

By combining experiments and simulations, a comprehensive understanding of the LFR prototype's performance was obtained, encompassing its thermal characteristics, optical efficiency, and long-term behavior under varying conditions. This information is invaluable for optimizing the design and operation of the LFR prototype for enhanced solar energy harvesting.

III. RESULTS AND DISCUSSION

Ambient conditions play a critical role in the prototype's performance. The essay was conducted on January 6th, 2023, under climatic conditions of Agadir city in Morocco. This day was selected for its favorable weather conditions, featuring a mostly clear sky with minimal cloud cover. Fig.14 shows the variations in ambient temperature and solar radiation intensity during the testing day.

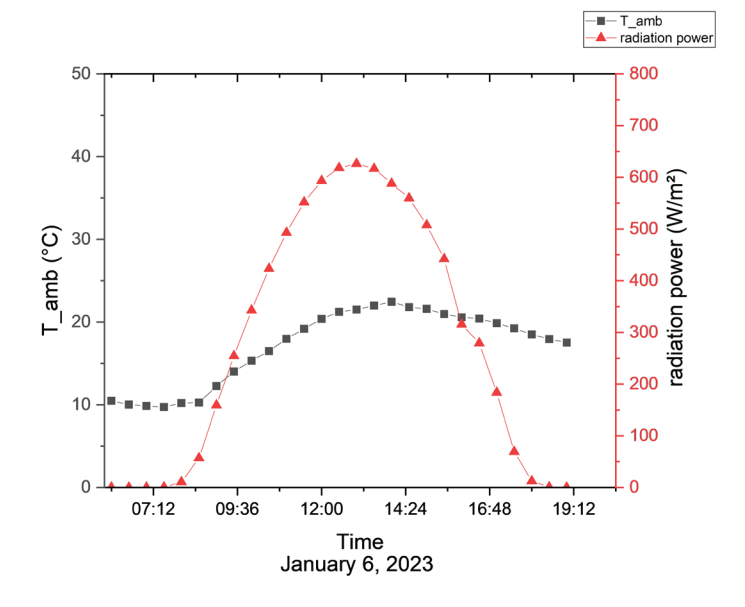


Fig. 14. Evolution of ambient temperature and solar radiation over the testing day

As shown in Fig. 14, solar radiation intensity gradually increased from the morning and reached a peak of 626 W/m² around midday before progressively declining until sunset. The ambient temperature pursued a similar trend, starting at 10°C in the early morning, rising to 23°C at noon, and then decreasing to 17°C by the end of the day. The average ambient temperature throughout the day was 19.23°C.

A. Stagnation Temperature Determination

Several experiments were conducted in order to assess the stagnation temperature of the prototype. These conducted tests aim to assess the parameter U_r , evaluate the optimal operating temperature of the LFR prototype, and estimate the collector's efficiency. The results of the experiment carried out on January 6, 2023, are presented (Fig. 15). The curve deals with the temporal variation of the receiver surface temperature. The stagnation temperature of the heat transfer fluid can be derived from the recorded surface temperature data. The LFR system was sun-exposed to solar irradiation during clear skies. Throughout the test time, from 01:30 PM to 02:00 PM, the ambient temperature and the average of solar radiation were 23 °C and , $625 W/m^2$ respectively.

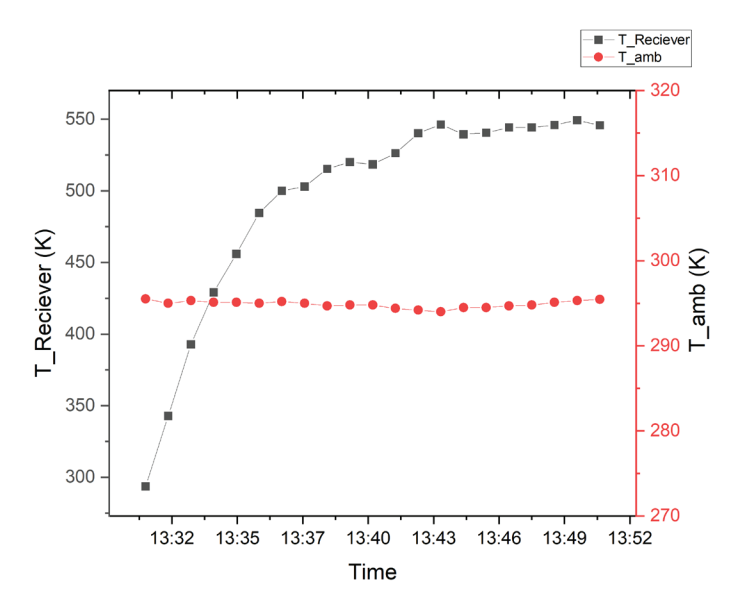


Fig. 15. The evolution of the receiver temperature until reaching the stagnation value

The curve in Fig. 15 shows that the receiver surface temperature increases significantly during about the first 12 min of sun exposure then the evolution of the temperature tends to be slight. The absorber reaches an asymptotically stable state in approximately 20 minutes, attaining a stagnation temperature of 536 K (263°C).

Fig. 16 presents the variation of the stagnation temperature as a function of the concentration ratio [29].

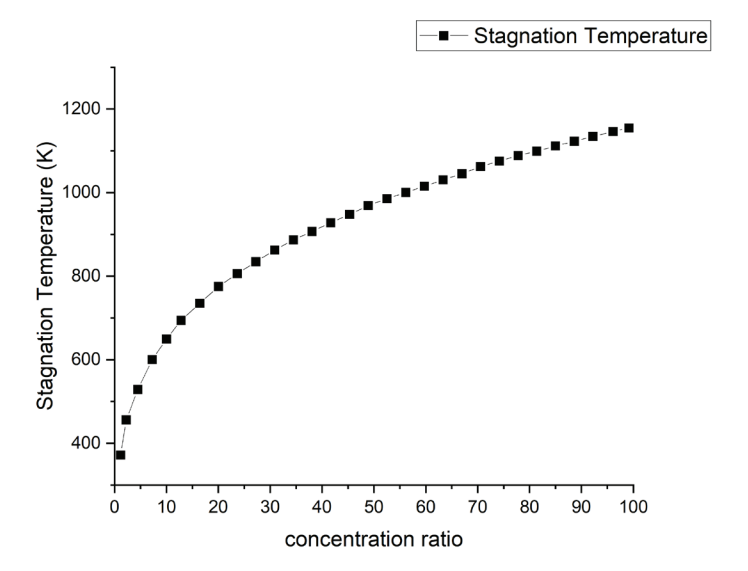


Fig. 16. The stagnation temperature depending on the concentration ratio

By simply projecting our measured stagnation temperature value on the theoretical curve, we can realize that our concentration ratio is 6, in other words. 6 times the sun or six suns.

The optimal operating temperature of the LFR system is derived from the following equation [28]:

$$T_{op} = \sqrt{Tstag.Tamb} \sim 398K = 125°C$$
 (12)

Overall, our prototype offers interesting performance, with a high stagnation temperature (263°C) and a moderate concentration ratio (6 suns). The operating temperature (125°C) is suitable for several applications, especially for the MED distillation process.

Concerning the heat transfer coefficient (U_r) of the prototype under the mentioned conditions, the average values, as deduced from Eq. (7), and using of the measurable parameters during the ($q^* = 625 \, W/m^2$, $T_0 = 296 \, K$, and concentration ratio C = 8.8), U_r is found to be close to $23 \, W/m^2 K$.

The receiver can be characterized through the stagnation parameter expressed by Eq. (13) [30]:

$$Y = (T_{rmax} - T_0)/q^* (13)$$

By incorporating the overall heat transfer coefficient defined in (Eq.(7)), the stagnation parameter can be written as $Y=C/U_r$. The calculation of this parameter in our case was determined to be 0.38 m2.K/W. Under comparable test

conditions, the GB/T 1709-2005 standards of China specify a minimum value of stagnation parameter in $0.19 \, \text{m}^2$.K/W, which is significantly lower than our obtained value.

It is noteworthy to reference the findings of Lin et al. [31], in which this parameter was found to be 0.34 m².K/W, closely aligning with our own results.

In order to estimate the collector's efficiency at an operating temperature of 125°C, following Eq. (10):

$$\eta_c = 1 - \frac{U_r(T_{op} - T_0)}{q * . C}$$
 $\eta_c = 0.56 = 56\%$

A collector's efficiency of 56% for the tested LFR prototype is recorded at an operating temperature of 125°C. This remarkable value is achieved despite the fact that collector efficiency generally decreases with increasing fluid temperature. This result proves the suitability of this technology for converting solar energy into thermal energy under the climate conditions of our region.

B. Optical Efficiency Measurement

The optical efficiency of our prototype is evaluated by measuring the incident light power on the horizontal plane (plane mirror) and that reaching the receiver plane. Table II summarizes the measured values for each reflector:

TABLE II. MEASURED VA	LUES FOR	EACH N	MIRROR
-----------------------	----------	--------	--------

	M1	M2	МЗ	M4	M5	M6	M7	M8	М9	M10	M11
Horizontal plane (W/m²)	587	534	561	486	594	554	462	576	536	514	528
Receiver plane (W/m²)	398	320	342	315	386	354	279	368	332	334	332

Therefore, experimentally, the average optical efficiency of the concentrator:

$$<\eta_{opt}> = 0.62 = 62\%$$

This result is comparable to the theoretical analysis of the LFR system of Rajendran et al. [32] in their study related to the effect of the concentrator aperture area of the collector on the concentrated power reached to the tubular absorber. They estimated that the solar energy availability was 62.5% at a concentration ratio of 8.31.

An optical efficiency of 0.62 indicates that the concentrator has an intermediate optical efficiency. Losses can be due to several factors, such as Reflections on mirror surfaces, Absorption by concentrator materials, Light scattering, and Mirror positioning error.

It is important to highlight that limited attention, as mentioned previously, has been given in earlier studies to the design of small-scale LFR systems optimized for decentralized use, particularly in combination with MED units operating in remote or economically constrained areas and particularly under the climate conditions of Morocco. These

results demonstrate the potential of such systems to provide an efficient and cost-effective thermal energy source under these specific conditions.

C. TRNSYS Simulation

We simulated an LFR system of the same size as our prototype, using historical weather data for Agadir City in Morocco. The curves of Fig. 17-18-19 show the evolution of the storage tank's inlet (red color curve) and outlet (blue color curve) temperatures over the path of the day (January 6th); the curve in pink color represents the solar radiation intensity. The curves plotted from simulations performed using TRNSYS have a very similar shape to those found experimentally by [33]. According to the simulation results, the LFR thermal performance over a day is affected by the tank size and the fluid flow rate.

In the first case (1st scenario, Fig.17), the system reaches a maximum outlet temperature of 126 °C after 6 hours of heating using a 37-liter tank and a 30 Kg/h flow rate. As a result of the higher thermal inertia and thus slower temperature rise, the larger tank volume takes much more time to reach its maximum temperature.

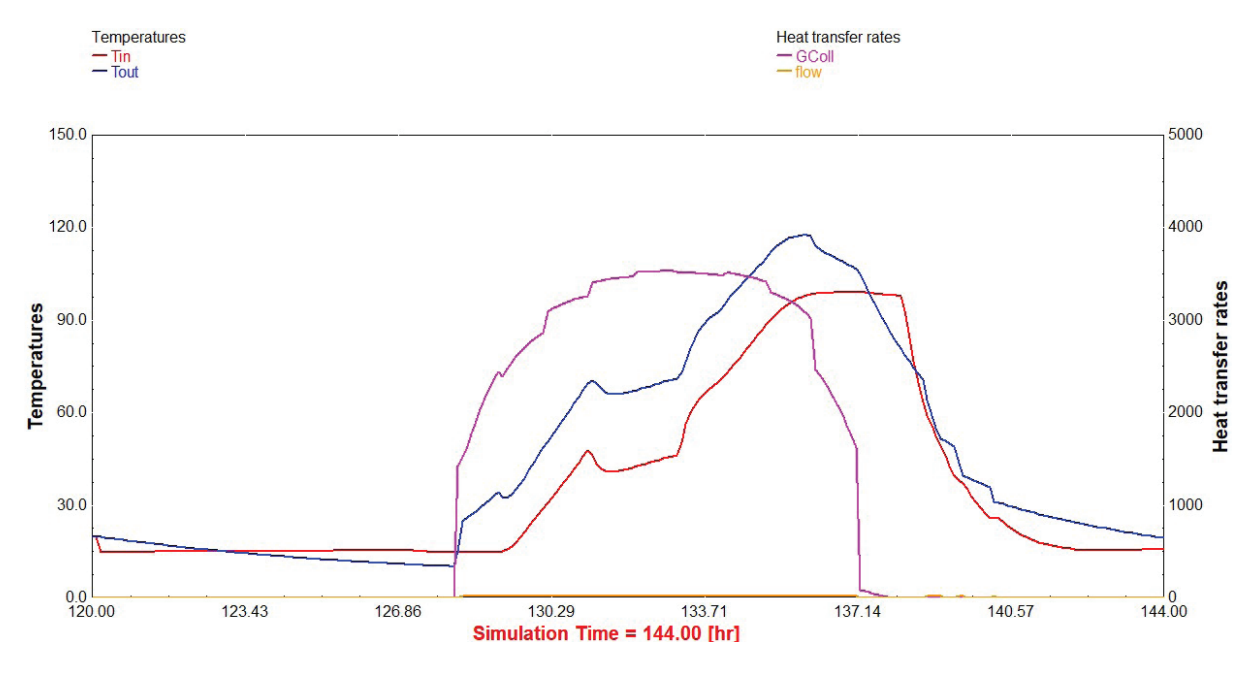


Fig.17. The evolution of the storage tank's inlet and outlet temperatures over the course of the day (1st scenario: 30Kg/h, 37L)

In the second scenario (Fig.18), the system reaches a peak output temperature of 124 °C in just three hours when the tank volume is decreased to 17-Liter while

keeping the same flow rate of 30 kg/h. Because of its lower thermal capacity, the smaller tank heats up more quickly than the bigger tank.

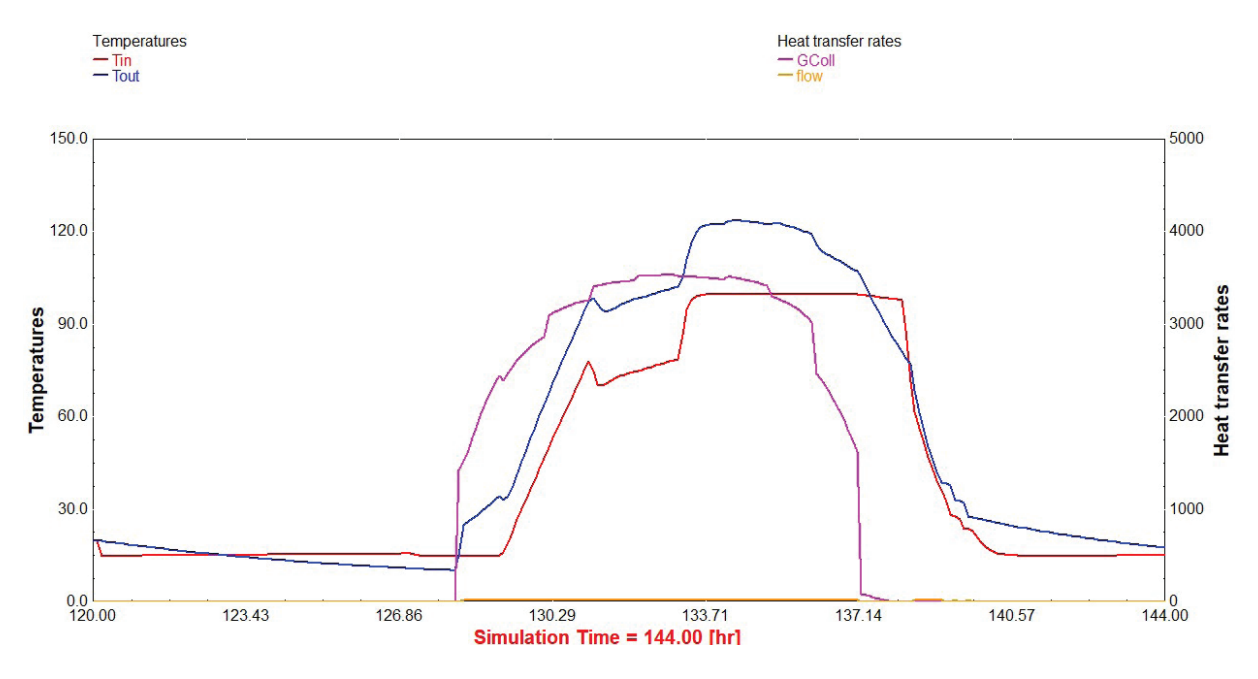


Fig.18. The evolution of the storage tank's inlet and outlet temperatures over the course of the day (2nd scenario: 30Kg/h, 17L)

Finally, in the third scenario (Fig.19), the maximum output temperature increases to 135 °C, again after three hours, using the smaller tank of 17-Liter and

a lower flow rate of 20 kg/h. A greater peak outlet temperature results from the fluid absorbing more heat per unit of time due to the reduced flow rate.

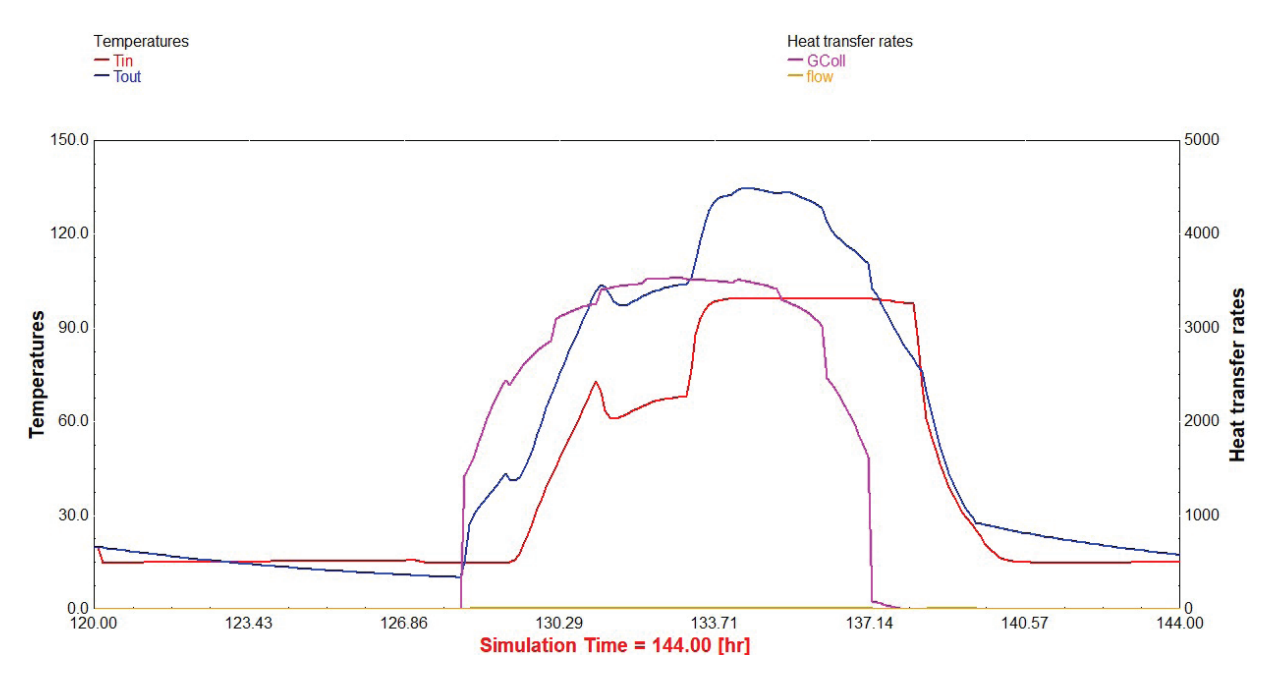


Fig.19. The evolution of the storage tank's inlet and outlet temperatures over the course of the day (3rd scenario: 20Kg/h, 17L)

According to this comparison, the system's thermal output is deeply influenced by both tank size and fluid flow rate, with smaller tanks and lower flow rates reaching higher temperatures in a shorter time. These results are useful for optimizing tank size and flow rates in solar thermal systems to achieve the required temperature outputs and efficiency.

IV. CONCLUSION

This study highlights the potential of Linear Fresnel Reflectors (LFRs) as an innovative and adequate technology for solar heat production. These systems show significant good characteristics in terms of simplicity, cost, and the use of locally available materials. They are designed to meet the specific needs of arid climate regions, such as Agadir in Morocco.

It is a practical contribution toward the advancement of small-scale, cost-effective LFR solutions suitable for decentralized use, particularly in conjunction with MED desalination systems. By targeting affordability and efficiency, the study supports the wider adoption of LFR technology in contexts where large-scale installations are not feasible.

This work aimed to explore the potential of LFRs intended to power multi-effect distillation (MED)

processes. The developed prototype integrates an innovative tubular absorber with an optimized thermal storage system. Experimental tests revealed encouraging performances, with a stagnation temperature reaching 263 °C, an overall heat transfer coefficient of $23\ W/m^2K$, and a collector's efficiency of 56% at an operating temperature of 125 °C. Numerical simulations performed using TRNSY software confirmed that the thermal performances of the system strongly depend on parameters such as the storage tank size and the fluid flow rate.

These results demonstrate that linear Fresnel reflectors (LFRs) might be a reliable and sustainable solution to supply thermal energy for cost-effective MED desalination processes. Such a device offers an affordable and technologically feasible alternative, especially for regions where access to local and renewable resources is crucial. Further optimization and integration labors are in progress to enhance the economic and environmental impact of these devices at a large scale.

Acknowledgment:

This study was supported by The Moroccan Ministry of Higher Education, Research and Innovation in the framework of (PPR/2015/31) project.

References

- [1] M. M. Mekonnen and A. Y. Hoekstra, "Sustainability: Four billion people facing severe water scarcity," *Sci Adv*, vol. 2, no. 2, 2016, doi: 10.1126/sciadv.1500323.
- [2] C. He et al., "Future global urban water scarcity and potential solutions," *Nat Commun*, vol. 12, no. 1, 2021, doi: 10.1038/s41467-021-25026-3.
- [3] A. Zyadin, "Water Shortage in MENA Region: An Interdisciplinary Overview and a Suite of Practical Solutions," *J Water Resour Prot*, vol. 05, no. 04, pp. 49–58, 2013, doi: 10.4236/jwarp.2013.54A008.
- [4] UNESCO, Chapter 2: Physical and environmental dimensions. 2019.
- [5] S. Almasoudi and B. Jamoussi, "Desalination technologies and their environmental impacts: A review," *Sustainable Chemistry One World*, vol. 1, 2024, doi: 10.1016/j.scowo.2024.100002.
- [6] S. Manju and N. Sagar, "Renewable energy integrated desalination: A sustainable solution to overcome future fresh-water scarcity in India," 2017. doi: 10.1016/j.rser.2017.01.164.
- [7] N. Voutchkov, "Energy use for membrane seawater desalination current status and trends," 2018. doi: 10.1016/j.desal.2017.10.033.
- [8] D. Zarzo and D. Prats, "Desalination and energy consumption. What can we expect in the near future?," *Desalination*, vol. 427, 2018, doi: 10.1016/j.desal.2017.10.046.
- [9] M. Shatat, M. Worall, and S. Riffat, "Opportunities for solar water desalination worldwide: Review," 2013. doi: 10.1016/j. scs.2013.03.004.
- [10] M. Alhajand S. G. Al-Ghamdi, "Reducing electric energy consumption in linear Fresnel collector solar fields coupled to thermal desalination plants by optimal mirror defocusing," *Heliyon*, vol. 4, no. 9, 2018, doi: 10.1016/j.heliyon.2018. e00813.
- [11] I. B. Askari and M. Ameri, "Techno economic feasibility analysis of Linear Fresnel solar field as thermal source of the MED/TVC desalination system," *Desalination*, vol. 394, 2016, doi: 10.1016/j.desal.2016.04.022. http://a

- [12] A. E. Rungasamy, K. J. Craig, and J. P. Meyer, "A review of linear Fresnel primary optical design methodologies," *Solar Energy*, vol. 224, pp. 833–854, Aug. 2021, doi: 10.1016/j. solener.2021.06.021.
- [13] M. Babu, S. S. Raj, and A. Valan Arasu, "Experimental analysis on Linear Fresnel reflector solar concentrating hot water system with varying width reflectors," *Case Studies in Thermal Engineering*, vol. 14, p. 100444, Sep. 2019, doi: 10.1016/j.csite.2019.100444.
- [14] STS-med, "Concentrated Solar Thermal Energy Systems Handbook," *Energy Sources*, 2016.
- [15] N. B. Desai and S. Bandyopadhyay, "Integration of parabolic trough and linear Fresnel collectors for optimum design of concentrating solar thermal power plant," *Clean Technol Environ Policy*, vol. 17, no. 7, pp. 1945–1961, Oct. 2015, doi: 10.1007/s10098-015-0918-9.
- [16] J. Sun, Z. Zhang, L. Wang, Z. Zhang, and J. Wei, "Comprehensive Review of Line-Focus Concentrating Solar Thermal Technologies: Parabolic Trough Collector (PTC) vs Linear Fresnel Reflector (LFR)," Journal of Thermal Science, vol. 29, no. 5, pp. 1097–1124, Oct. 2020, doi: 10.1007/s11630-020-1365-4.
- [17] A. Ahmadpour, A. Dejamkhooy, and H. Shayeghi, "Optimization and modelling of linear Fresnel reflector solar concentrator using various methods based on Monte Carlo Ray-Trace," *Solar Energy*, vol. 245, pp. 67-79, Oct. 2022, doi: 10.1016/j.solener.2022.09.006.
- [18] M. Alhaj, F. Tahir, and S. G. Al-Ghamdi, "Lifecycle environmental assessment of solar-driven Multi-Effect Desalination (MED) plant," *Desalination*, vol. 524, p. 115451, Feb. 2022, doi: 10.1016/j.desal.2021.115451.
- [19] M. Alhaj, A. Mabrouk, and S. G. Al-Ghamdi, "Energy efficient multi-effect distillation powered by a solar linear Fresnel collector," Energy Convers Manag, vol. 171, pp. 576–586, Sep.2018,doi:10.1016/j.enconman.2018.05.082.
- [20] O. K. Buros, *ABCs1.pdf*, 2nd edition., vol. Int. Desalin. Assoc. 2000.

- [21] A. Parikh, J. Martinek, G. Mungas, N. Kramer, R. Braun, and G. Zhu, "Investigation of temperature distribution on a new linear Fresnel receiver assembly under high solar flux," *Int J Energy Res*, vol. 43, no. 9, pp. 4051–4061, Jul. 2019, doi: 10.1002/er.4374.
- [22] S.S.Mathur, T.C.Kandpal, and B.S.Negi, "Optical design and concentration characteristics of linear Fresnel reflector solar concentrators—II. Mirror elements of equal width," *Energy Convers Manag*, vol. 31, no. 3, pp. 221–232, Jan. 1991, doi: 10.1016/0196-8904(91)90076-U.
- [23] E. Bellos, "Progress in the design and the applications of linear Fresnel reflectors A critical review," *Thermal Science and Engineering Progress*, vol. 10, pp. 112–137, May 2019, doi: 10.1016/j.tsep.2019.01.014.
- [24] A. Buscemi, D. Panno, G. Ciulla, M. Beccali, and V. Lo Brano, "Concrete thermal energy storage for linear Fresnel collectors: Exploiting the South Mediterranean's solar potential for agri-food processes," *Energy Convers Manag*, vol. 166, pp. 719–734, Jun. 2018, doi: 10.1016/j. enconman.2018.04.075.
- [25] "Heat Transfer Fluids | Therminol | Eastman." [Online]. Available: https://www.therminol.com/heat-transfer-fluids
- [26] "Portable Handheld Data Logger," 2023. [Online]. Available: https://sea.omega.com/tw/pptst/OM-DAQPRO-5300.html
- [27] "Solar Power Meter (Datalogging) TES-132 |TES Electrical Electronic Corp.," 2025. [Online]. Available: https://www.tes.com.tw/en/ product_detail.asp?seq=284

- [28] S. A. Kalogirou, *Solar energy engineering: Processes and systems.* 2009. doi: 10.1016/B978-0-12-374501-9.X0001-5.
- [29] J.B.Rapsodee,P.Pascal,S.Latep,andC.Doctorale, "Cogénération héliothermodynamique avec concentrateur linéaire de Fresnel: modélisation de l'ensemble du procédé".
- [30] Y. Zhiqiang, "Development of solar thermal systems in China," *Solar Energy Materials and Solar Cells*, vol. 86, no. 3, pp. 427–442, Mar. 2005, doi: 10.1016/j.solmat.2004.07.012.
- [31] M. Lin, K. Sumathy, Y. J. Dai, R. Z. Wang, and Y. Chen, "Experimental and theoretical analysis on a linear Fresnel reflector solar collector prototype with V-shaped cavity receiver," *Appl Therm Eng*, vol. 51, no. 1–2, pp. 963–972, Mar. 2013, doi: 10.1016/j. applthermaleng.2012.10.050.
- [32] M. Rajendran and A. Valan Arasu, "Design and performance characteristics analysis of a linear fresnel reflector solar concentrator system with a trapezoidal cavity absorber," International Journal of Emerging Technology and Advanced Engineering, vol. 10, no. 5, 2020.
- [33] E. Bellos, E. Mathioulakis, E. Papanicolaou, and V. Belessiotis, "Experimental investigation of the daily performance of an integrated linear Fresnel reflector system," *Solar Energy*, vol. 167, pp. 220–230, Jun. 2018, doi: 10.1016/j. solener.2018.04.019.